Dynamics of C_2 formation in laser-produced carbon plasma in helium environment

K. F. Al-Shboul, S. S. Harilal,[a] A. Hassanein, and M. Polek
School of Nuclear Engineering and Center for Materials Under Extreme Environment, Purdue University, 400 Central Dr., West Lafayette, Indiana 47907, USA

(Received 20 December 2010; accepted 21 January 2011; published online 9 March 2011)

We investigated the role of helium ambient gas on the dynamics of C_2 species formation in laser-produced carbon plasma. The plasma was produced by focusing 1064 nm pulses from an Nd:YAG laser onto a carbon target. The emission from the C_2 species was studied using optical emission spectroscopy, and spectrally resolved and integrated fast imaging. Our results indicate that the formation of C_2 in the plasma plume is strongly affected by the pressure of the He gas. In vacuum, the C_2 emission zone was located near the target and C_2 intensity oscillations were observed both in axial and radial directions with increasing the He pressure. The oscillations in C_2 intensity at higher pressures in the expanding plume could be caused by various formation zones of carbon dimers. © *2011 American Institute of Physics*. [doi:10.1063/1.3555679]

I. INTRODUCTION

Carbon laser-produced plasmas (LPP) have received a great attention over the last few years because of its numerous technological applications that include diamond-like carbon (DLC) deposition and nanostructures production (carbon nanotubes, nanowires, and graphene).[1,2] It is well known that carbon giant clusters, C_{60} and higher fullerenes, are known to be produced by the laser ablation of carbon in the presence of an ambient helium atmosphere.[3] However, the mechanism which leads to formation of nanotubes and nanocluster growth in laser ablation plumes is yet to be fully understood. Hence, it is still a great uncertainty as to when and where the carbon clusters are formed within the laser-ablated plume. The way the ablated plume interacts with the ambient gas strongly affects the nature of carbon clusters production. This indicates that more fundamental studies are essential to fully understand these mechanisms and how to generate nanotubes with well-defined structures or synthesis of bulk high quality nanotubes.

In the context of carbon clusters and nanotubes, it is articulated that the molecular C_2 plays a prominent role in their formation where carbon giant molecules are assumed to be created by chaining of C_2 molecules. Van Orden and Saykally[4] reported that C_2 dimers might be the precursors to nanotube growth. Motaung *et al.*[5] reported the role of C_2 in synthesizing single walled carbon nanotubes (SWCNTs) and noticed large fluctuations in C_2 intensity due to the nucleation and rapid growth of SWCNTs. Moodley and Coville[6] found that one laser-shot was enough to ablate sufficient material for the SWCNTs nucleation and noticed that C_2 emission starts directly after the onset of ablation. Camacho *et al.*,[7] using CO_2 laser excitation, found that C_2 emission increases with increasing ambient air pressure up to 1.5 Torr, but beyond this pressure, they noticed a decrease in the time-integrated emission intensity of C_2. They suggested that this reduction in intensity was due to shielding by the air plasma, where a part of the long laser energy pulse is absorbed by the air plasma during its expansion. Yamagata *et al.*[8] noticed atomic and ionic species contribution to line emission from carbon plasma in vacuum, while C_2 Swan band and CN emission predominate when the plasma expanded into nitrogen ambient and suggested that the C_2 molecules are not ejected from the target but are formed in the plasma plume mainly by recombination.

Laser ablation has the unique advantage that most of the molecules are formed in their excited states, and hence, spectroscopic measurements offer an excellent means to investigate their evolution and dynamics.[9,10] Hence, LPP evolution and its species dynamics have been studied and monitored extensively in the past using various spectroscopy diagnostic tools; among these techniques are optical emission spectroscopy (OES),[11,12] laser-induced florescence (LIF),[13] optical emission spectroscopy time-of-flight measurements,[14,15] and fast intensified charge coupled device (ICCD) photography.[16–19] In this article, we report on the dynamics of C_2 species in laser ablated carbon plumes using emission spectroscopy and monochromatic fast photography. We investigated the effects of helium pressure on carbon plasma and the formation of C_2 molecules. Plume splitting and C_2 emission intensity oscillations in helium environment at different pressures have been observed.

II. EXPERIMENTAL SETUP

The experimental setup is schematically shown in Fig. 1. For producing plasmas, planar carbon targets (graphite, Alfa Aesar) mounted inside a stainless steel vacuum chamber were used. The chamber was pumped down to a base pressure of about 10^{-6} Torr using a turbo-molecular pump. The chamber was then filled with helium gas at pressures ranging from vacuum to 5 Torr. To produce plasma, the carbon targets were irradiated with 1064 nm pulses from a Nd:YAG (Continuum Surelite III) laser. This laser can be operated at a maximum repetition rate of 10 Hz with 6 ns full width half maximum.

[a]Electronic mail: sharilal@purdue.edu.

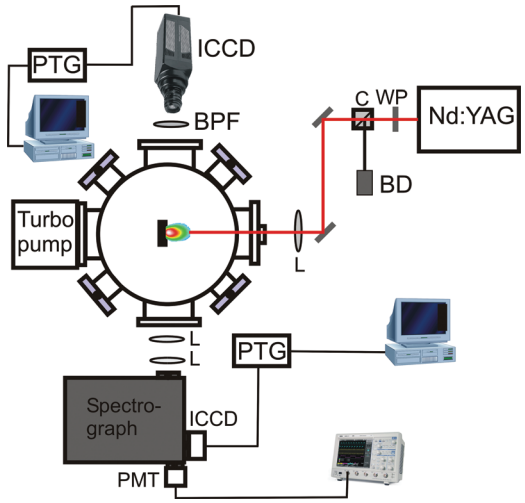

FIG. 1. (Color online) The schematic of experimental setup used in the present studies is given. (WP, wave plate; C, polarizing cube; BD, beam dump; L, lens; BPF, bandpass filter; and PTG, programmable timing generator).

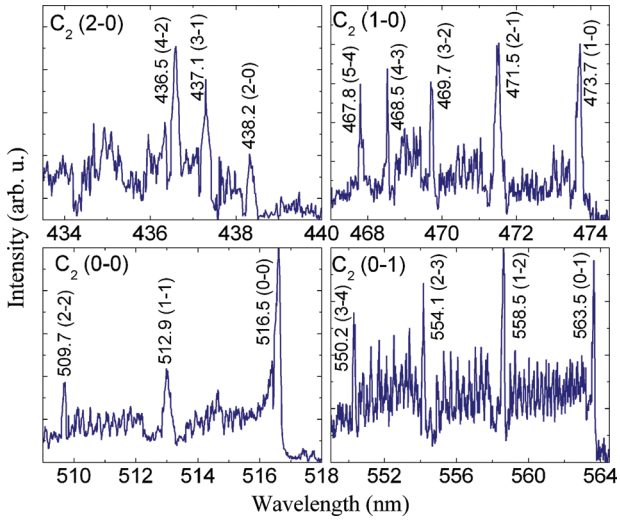

FIG. 2. (Color online) The spectra of C_2 Swan band for $\Delta v = 0, -1, 1$, and 2 are given.

To control the laser beam intensity, a combination of half wave plate and cube beam splitter was used. A programmable timing generator with overall temporal resolution of 1 ns and photodiodes (to monitor the onset of each laser shot) were used to synchronize the timing for all electronics during the experiments. The laser beam was focused on the target using anti-reflective-coated plano-convex lens and the estimated laser fluence at the target surface was 50 J cm^{-2}. To avoid target drilling, the target was continuously shifted using stepper motors. The OES was performed using a 0.5 m spectrograph (Acton SP-2500i) equipped with three gratings. The emission from the plasma was collected and imaged onto the spectrograph slit using appropriate collimating and focusing lenses in order to have one-to-one correspondence with the sampled area of the plasma and the image. This optical system was translated to monitor different parts of the plume. The spectrograph contains two exit ports. One of the exit ports was coupled to an intensified charged coupled device (ICCD, Princeton Instruments, Model Pi-MAX) for multichannel detection while a photomultiplier tube (PMT, Hamamatsu R928) is connected to the other exit port for single channel detection. A diverter mirror was used for switching between the PMT and the ICCD. The 2-D plume imaging was accomplished by positioning the ICCD orthogonal to the plasma expansion direction. Time integrated OES was performed in the visible region of the plasma. In order to discriminate C_2 molecules from other species, a bandpass filter was used for filtering (0-0) C_2 Swan band transition at 516 nm with 2 nm bandwidth.

III. RESULTS AND DISCUSSION

A. C_2 Swan band optical emission spectroscopy

Optical emission spectroscopic studies of laser produced carbon plume showed strong emission from carbon dimers along with neutral and lower-charged ions. Typical Swan band emission corresponding to transitions between the $d^3\Pi_g$ and $a^3\Pi_u$ electronic states[20,21] of the C_2 molecules for $\Delta v = -1$, 0, 1 and 2 are given in Fig. 2. These spectra were recorded at a distance of 1 mm from the target with an integration time of 2 μs and a laser fluence of 50 J cm^{-2} when the plume expanded freely into vacuum. The strongest emission was observed for the (0-0) transition at 516.5 nm. In vacuum, the emission features of C_2 were noticed only at short distances from the target surfaces (less than 3 mm). Yamagata *et al.*[8] noticed the absence of C_2 emission from carbon plasma in vacuum during their measurement. However, their measurements were made at a distance 10 mm from the target surface. Iida and Yeung[22] reported that the dominant mechanism for the production of C_2 molecules at low laser irradiance is likely to be the collision of electrons with clusters of higher numbers of carbon atoms followed by photo-fragmentation whereby one of the emitted product species is an excited C_2 molecule, whereas at higher irradiance Swan band emission is mainly due to excitation resulting from electron–ion and ion–ion recombination.

He ambient was added to the chamber to enhance the emission from carbon dimers. The presence of He ambient gas during plasma expansion causes the plume to be more emitting due to efficient electron impact excitation and plasma recombination. It should be remembered that for the production of carbon nano-clusters, an ambient is always used for controlling the plume expansion dynamics leading to enhanced cooling.[23] An ambient gas is also used for slowing down the energetic particles in making of DLC thin films.[8,24,25] Figure 3 shows the dependence of C_2 emission intensity on helium pressure at two distances from the target surface where time integrated line intensities of C_2 transition at 516.5 nm were used in this analysis. It clearly can be seen that C_2 emission intensity increases considerably with increasing the ambient helium pressure, especially above 100 mTorr. We also noticed that the extension of C_2 emission is considerably increased with the addition of He gas to the chamber. In vacuum, the C_2 emission is noticed only up to 3 mm from the target while with increasing pressure; the extension of C_2 emission is increased for further distances from the target surface.

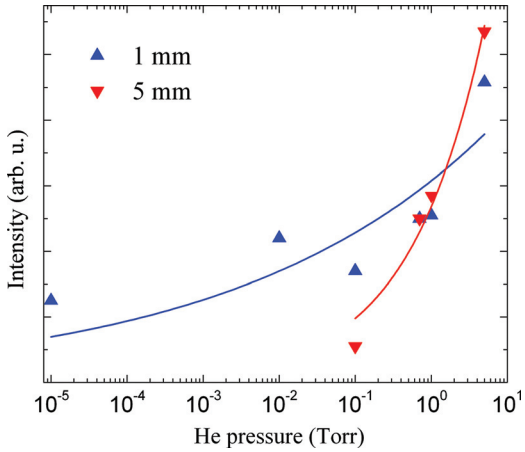

FIG. 3. (Color online) The dependence of optical emission intensity of (0-0) C_2 Swan band at $\lambda = 516.5$ nm on helium pressure. An integration time of 2 μs was used.

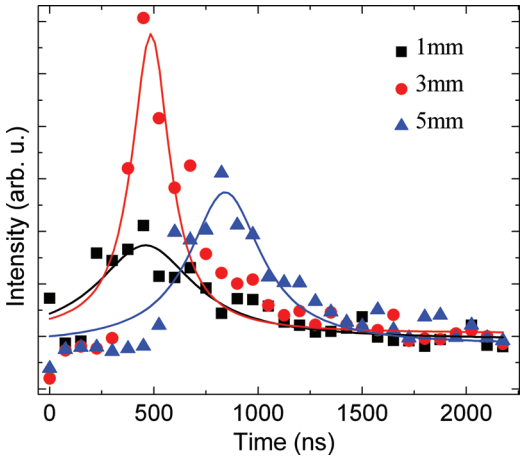

FIG. 5. (Color online) Time evolution of C_2 emission intensity at various distances from the target. The C_2 (0-0) transition at 516.5 nm was used for this measurement with an integration time of 50 ns.

We also investigated the effect of He ambient on both temporal and spatial features of C_2 emission. In our experiment, 2 μs time integrated spatial profiles of C_2 Swan band emission spectra from the 516.5 nm (0-0) transition were captured at 0.1, 0.4, and 0.7 Torr He pressures and at various distances from the target surface as shown in Fig. 4. The spatial analysis showed that the C_2 emission intensity reaches a peak at a specific distance from the target at a particular pressure and laser fluence. We also found that initially the C_2 maximum intensity location moves away from the target with a slight pressure increase. This effect can be explained by the more efficient cooling of the plasma at the plume front by the interaction with the ambient gas leading to more recombination of carbon atomic and ionic species.[26] However, at higher pressures, the peak location moves closer to the target possibly due to plasma confinement.

For the temporal analysis of the Swan bands of C_2, the emission spectra from the (0-0) transition were recorded at 1, 3, and 5 mm away from the target surface at 0.7 Torr He pressure by varying the delay times with respect to the laser pulse up to 2 μs with a fixed gate width of 50 ns which is shown in Fig. 5. The time resolved emission intensity constructed from these emission profiles showed large fluctuations that made it difficult for us to find the peaks of emission intensity. Each point in the figure is obtained from a single laser shot and the fluctuation in C_2 intensity could be due to the short gating time. Nevertheless, it is clear from the figure that the emission characteristics of C_2 vary drastically with time. The emission intensity increases initially with time at each distance studied where it peaks around a maximum value and after that starts to decay and almost vanishes after 2 μs. The C_2 emission exists for long times compared to 102 ns (C_2's natural lifetime for the $d^3\Pi_g$ state), which means that these molecules were formed by other mechanisms besides the ablation directly from the target surface such as collisional recombination during plasma cooling.[27] More studies employing time-of-flight emission spectroscopy[28,29] are essential to get a better insight of C_2 expansion dynamics which will be conducted in our future work.

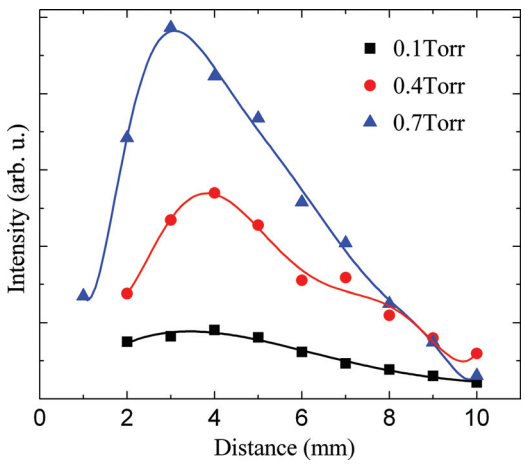

FIG. 4. (Color online) Spatial profiles of C_2 Swan band emission at various helium pressures. The C_2 (0-0) transition at 516.5 nm was used for this measurement with an integration time of 2 μs.

B. Spectrally integrated and resolved fast imaging

The time resolved imaging diagnostic tool has the advantage over other techniques that it gives a complete picture of the expansion dynamics of the plasma evolution by providing information about the plume evolution. In addition, by using narrow bandpass filters (BPFs), ICCD imaging can be used to distinguish contributions of various emitting species in the plume and identify their emission zones in the plasma. We recorded spectrally-integrated and monochromatic images of the expanding carbon plasma plume for understanding when and where the C_2 dimers are formed in laser-produced carbon plasma. Moreover, imaging the overall visible emission from the whole plasma plume helps to obtain information on the interaction of plasma with the ambient gas during earlier and later stages of the process. For obtaining monochromatic images, a narrow bandpass filter at 516 nm with 2 nm bandwidth was used. Our emission spectroscopic analysis showed that the (0-0) C_2 transition is the only vibrational emission line in this narrowband region.

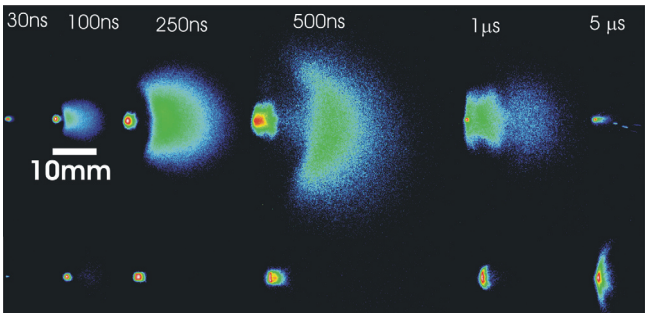

FIG. 6. (Color online) Spectrally-integrated (upper side) and C_2 monochromatic (lower side) images of carbon plasma in vacuum obtained using ICCD.

We recorded 2-D images of carbon plume at different times after the onset of plasma with a laser fluence of $50\,J\,cm^{-2}$ at different helium gas pressures ranging from 10^{-6} to 5 Torr. Both, the monochromatic and spectrally-integrated images were recorded using an ICCD camera. Typical spectrally-integrated and monochromatic plume images obtained in vacuum are given in Fig. 6. Each image is obtained from a single laser shot and all of the images presented in this work are normalized to the maximum intensity of that image for better clarity. A minimum gate width of 2 ns was used at the earliest time of plasma evolution and the gate width value was gradually incremented to higher values (2-100 ns) to compensate reduced emission at later stages of the plume life. The plume is found to expand freely in vacuum and nearly spherical in nature. A detachment of the fast moving emission zone can be seen even from 100 ns after the onset of plasma formation, commonly called plume splitting.[30] Plume splitting was extensively studied in the past and mainly observed at moderate pressure levels.[31,32] However, in our case plume splitting is also seen to be occurring in vacuum. The spectrally-filtered images showed the emission from C_2 is rather weak compared to spectrally-integrated images and most of the C_2 emission appeared at distances close to the target. A bright emission is noticed at the target surface even at delays greater than 1 μs.

Time resolved ICCD images of expanding carbon plume at various He pressures, both spectrally-integrated and monochromatic, are given in Fig. 7. An enhanced emission from C_2 species is distinctly seen from these ICCD images with increasing He pressure. A comparison between the spectrally-integrated and spectrally-resolved ICCD images at various He background pressures shows several interesting features. The shapes of the spectrally-integrated and monochromatic images are found to be different at lower pressures (e.g., 100 mTorr), while showing similarities at higher pressures. The main C_2 emission zone is limited to shorter distances at lower pressures (100 mTorr) especially at times <1 μs. This is due to lack of recombination of carbon species with high kinetic energies. In LPP, the velocity of the ions is dependent on their charge state and highly charged ions move with faster expansion velocity. The ions located at the front of the plasma acquire the largest energy during hydrodynamic acceleration and the interaction time for recombination is very much reduced. At higher pressures, the emission

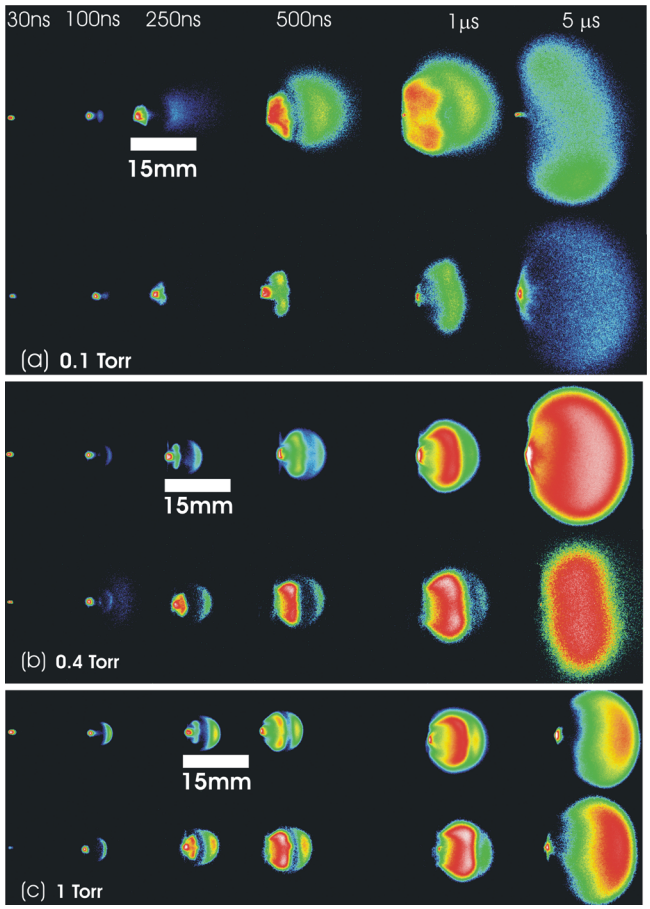

FIG. 7. (Color online) Spectrally-integrated (upper side) and C_2 monochromatic (lower side) images of carbon plasma at different He ambient pressures (a) 0.1, (b) 0.4, and (c) 1 Torr of helium gas pressure.

spatial distribution of C_2 is similar to the spectrally-integrated image and it shows that C_2 is the dominant for the emission in the plasma.

The monochromatic images showed that the distribution of C_2 is not uniform in the plume and it is more localized at various points in the plume. The lack of uniformity in C_2 emission could be due to various formation mechanisms of C_2 species.[22] Motaung *et al.*[5] also noticed large fluctuations in C_2 intensity at the optimum conditions for SWCNTs production. They indicated that the decrease in C_2 peak intensities followed by an increase in electron densities and electron temperature was due to the nucleation and rapid growth of SWCNTs. The emission intensity of C_2 as a function of distance along the direction of plume expansion is given in Fig. 8 for various He pressures at 250 ns after the onset of the plasma plume. The spatial analysis of C_2 emission clearly shows oscillations in intensity. The observed spatial feature is entirely different from data obtained from OES (Fig. 4) due to the differences in time integration and averaging over the line-of-sight (spectrograph slit height) in the OES measurements. Three C_2 maxima are seen in these profiles where two of them occurred closer to the target and the other one at the plume front.

The fastest intensity maxima occurred at farthest distance (plume front) may have been caused by increased recombination due to interaction between the expanding

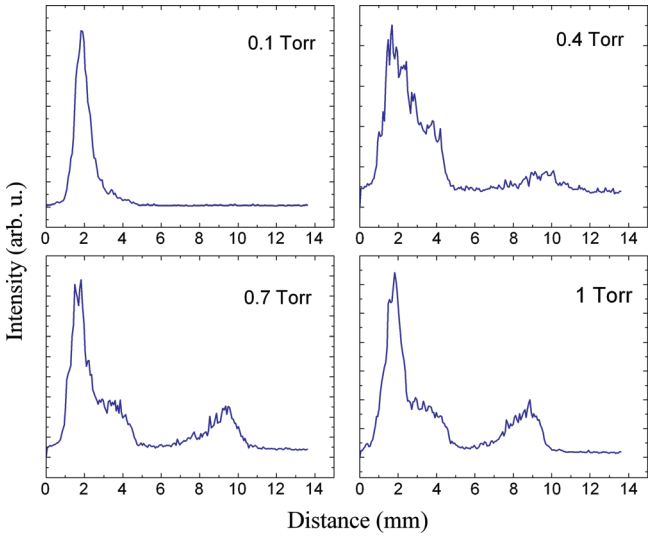

FIG. 8. (Color online) C_2 intensity counts obtained from filtered ICCD images (recorded at 250 ns after the onset of plasma formation) along the plume expansion direction at various He pressures.

plume and ambient gas. However, the C_2 emission that occurred in the mid-plume which corresponds to the slower peak is rather difficult to explain. Yadav *et al.*[33] noticed similar plume bifurcation during LIF studies of C_2 species and attributed this effect to recombination of slow moving carbon species and formation of nanoparticles.

We have also observed oscillations in C_2 intensity in the radial direction (perpendicular to plasma expansion direction). The radial emission profiles of C_2 are given in Fig. 9. The C_2 emission intensity at the center of plasma (closest to the target surface) is relatively smaller than the plasma radial peripheries (plasma wings) with the introduction of helium gas pressure that could be due to the dissociation of C_2 molecules caused by collisional effects with the energetic atomic and ionic species in the center region of the ablated plasma. Previous studies showed that the particles with higher kinetic energy are emitted closer to the target surface normal and their concentration falls sharply away from the normal.[34]

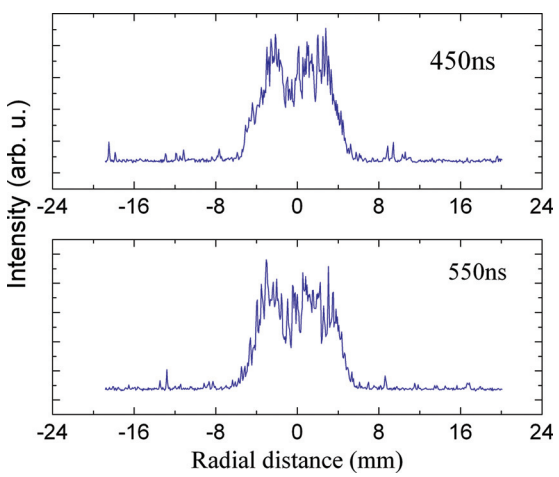

FIG. 9. (Color online) The C_2 radial intensity profiles at 4 mm away from the target surface at 0.1 Torr of helium gas pressure obtained from the monochromatic ICCD images. The times given are after the onset of plasma formation.

Hence, more recombination is favored in the wings rather than at the center of the plume which could be the reason for the asymmetrical C_2 radial profile.

Both the monochromatic and the spectrally-integrated ICCD images show plume splitting, indicating that the plasma plume consists of multiple components. By comparing the images, the oscillations in intensity seen in the spectrally-integrated images could be caused by various formation zones of carbon dimers. The ICCD images can be used for getting better insights of C_2 species and plasma plume expansion dynamics. The position-time (R-t) plots obtained for both fast and slow intensity peaks from spectrally-integrated and monochromatic images for 0.4 and 1 Torr are given in Fig. 10. Peaks 1 and 2 in the figures correspond to the fast and slow moving intensity peaks in the ICCD images (the peaks seen in Fig. 8), respectively.

The plasma expansion in the presence of an ambient gas can be represented by the shock model[2] which is defined by $R = \xi_o (E_o/\rho_o)^{1/5} t^{2/5}$ where t is the delay time, E_o is the explosive release of energy, ρ_o is the ambient gas density, and ξ_o is a constant which depends on γ, the specific heat capacity. As shown in Fig. 10 the first component (Peak 1)

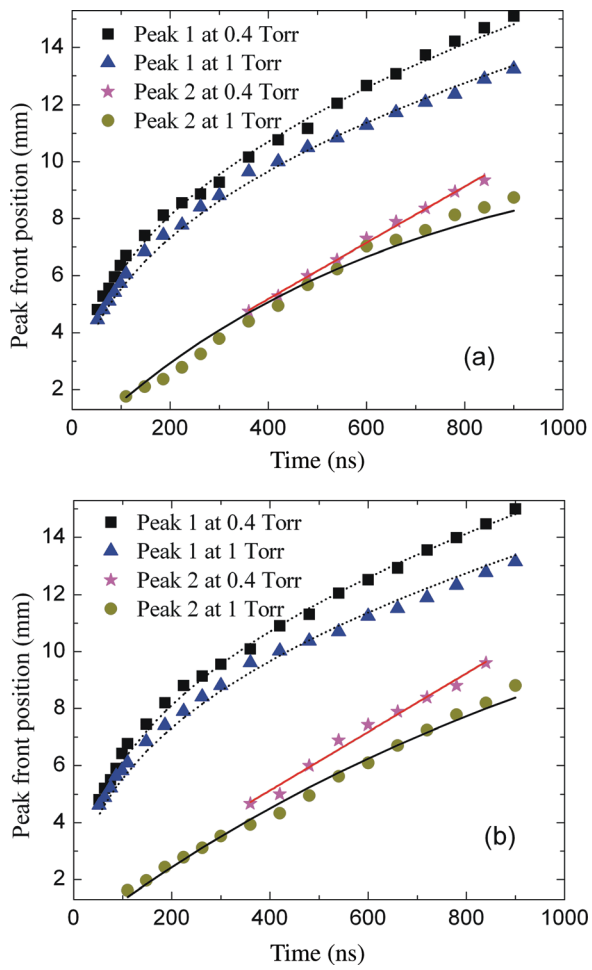

FIG. 10. (Color online) Position–time (*R-t*) plots of two front position peaks of the carbon plume produced at 0.4 and 1 Torr helium pressures measured from (a) spectrally-integrated and (b) monochromatic (with $\lambda = 516.5$ nm) ICCD plume images. The symbols represent experimental data points and curves represent different expansion models; the dotted curves represent the shock wave model ($R \propto t^{0.4}$). The solid curves show the drag model fit.

expansion in both images agrees well with the shock position model ($R \propto t^{0.4}$). However, we found that the shock model does not explain the expansion of the delayed component (Peak 2). At 0.4 Torr, this slower component is found to move linearly with time, while at higher pressures (1 Torr) the drag model[23] provides a better fit.

IV. CONCLUSIONS

We investigated the role of ambient helium gas pressure on the formation of carbon dimers in a laser-produced plasma. Optical emission spectroscopy and fast gated photography were used as diagnostics. The C_2 emission features were studied with ambient helium pressure ranging from 10^{-6} to 5 Torr. Filtered C_2 images of the plume employing narrow bandpass filter provided the location of C_2 emission zones in the plume.

Free expansion and splitting of the plume were observed at different pressure levels. Both OES and fast ICCD imaging show that C_2 emission is present in vacuum at early times and at short distances (less than 3 mm) and this emission can be enhanced and extended for longer times and further distances by introducing ambient helium pressure. Fast ICCD photography studies show oscillations in C_2 emission intensity both in axial and radial directions. The observation of fast moving C_2 species noticed in the plume front positions could be formed due to enhanced recombination caused by rapid cooling due to plume-ambient species interaction. The observed C_2 emission zones in the mid plume are caused by recombination of slow moving carbon species and/or dissociation of carbon clusters. A comparison between spectrally integrated and filtered images showed C_2 was the dominant emitting species at higher pressures. We compared the expansion dynamics of the plume with the shock expansion model and found the plume front is following $t^{0.4}$ dependence with space.

ACKNOWLEDGMENTS

This work was partially supported by the US DOE NNSA contract number DE-NA0000463 and the College of Engineering, Purdue University.

[1]E. Cappelli, C. Scilletta, G. Mattei, V. Valentini, S. Orlando, and M. Servidori, Appl. Phys. A **93**, 751 (2008).
[2]D. B. Geohegan, *Pulsed Laser Deposition of Thin Films* (Wiley, New York, 1994).
[3]R. E. Smalley, Accts. Chem. Res. **25**, 98 (1992).
[4]A. Van Orden and R. J. Saykally, Chem. Rev. **98**, 2313 (1998).
[5]D. E. Motaung, M. K. Moodley, E. Manikandan, and N. J. Coville, J. Appl. Phys. **107**, 044308 (2010).
[6]M. K. Moodley and N. J. Coville, Chem. Phys. Lett. **498**, 140 (2010).
[7]J. J. Camacho, M. Santos, L. Diaz, and J. M. L. Poyato, J. Phys. D. **41**, 215206 (2008).
[8]Y. Yamagata, A. Sharma, J. Narayan, R. M. Mayo, J. W. Newman, and K. Ebihara, J. Appl. Phys. **86**, 4154 (1999).
[9]A. M. Keszler and L. Nemes, J. Mol. Struc. **695**, 211 (2004).
[10]Y. Tasaka, M. Tanaka, and S. Usami, Jpn. J. Appl. Phys. **34**, 1673 (1995).
[11]H. Riascos, L. M. Franco, and J. A. Perez, Phys. Scr. **T131**, 014020 (2008).
[12]D. Campos, S. S. Harilal, and A. Hassanein, J. Appl. Phys. **108**, 113305 (2010).
[13]A. Okano and K. Takayanagi, J. Appl. Phys. **86**, 3964 (1999).
[14]S. S. Harilal, Appl. Surf. Sci. **172**, 103 (2001).
[15]R. W. Coons, S. S. Harilal, D. Campos, and A. Hassanein, J. Appl. Phys. **108**, 063306 (2010).
[16]S. Abdelli-Messaci, T. Kerdja, A. Bendib, and S. Malek, J. Phys. D **35**, 2772 (2002).
[17]J. J. Camacho, L. Diaz, M. Santos, L. J. Juan, and J. M. L. Poyato, J. Appl. Phys. **106**, 033306 (2009).
[18]A. Neogi and R. K. Thareja, Phys. Plasmas. **6**, 365 (1999).
[19]S. S. Harilal, J. Appl. Phys. **103**, 123306 (2007).
[20]R. W. B. Pearse and A. G. Gaydon, *The Identification of Molecular Spectra* (Chapman and Hall, London, 1965).
[21]W. Weltner and R. J. Vanzee, Chem. Rev. **89**, 1713 (1989).
[22]Y. Iida and E. S. Yeung, Appli. Spectros. **48**, 945 (1994).
[23]S. George, A. Kumar, R. K. Singh, and V. P. N. Nampoori, Appl. Phys. A **98**, 901 (2010).
[24]W. J. Liu, X. J. Guo, C. L. Chang, and J. H. Lu, Thin Solid Films **517**, 4229 (2009).
[25]Y. Yamagata, T. Ohshima, T. Ikegami, R. K. Thareja, K. Ebihara, A. Sharma, R. M. Mayo, and J. Narayan, Materials Research Society Symposium Proceedings **648**, P6.55 (2001).
[26]S. S. Harilal, B. O'Shay, Y. Tao, and M. S. Tillack, J. Appl. Phys. **99**, 083303 (2006).
[27]A. Kushwaha and R. K. Thareja, Appl. Opt. **47**, G65 (2008).
[28]S. S. Harilal, R. C. Issac, C. V. Bindhu, V. P. N. Nampoori, and C. P. G. Vallabhan, J. Appl. Phys. **81**, 3637 (1997).
[29]S. S. Harilal, R. C. Issac, C. V. Bindhu, V. P. N. Nampoori, and C. P. G. Vallabhan, J. Appl. Phys. **80**, 3561 (1996).
[30]S. S. Harilal, C. V. Bindhu, M. S. Tillack, F. Najmabadi, and A. C. Gaeris, J. Appl. Phys. **93**, 2380 (2003).
[31]S. Mahmood, R. S. Rawat, M. S. B. Darby, M. Zakaullah, S. V. Springham, T. L. Tan, and P. Lee, Phys. of Plasmas **17**, 103105 (2010).
[32]R. F. Wood, K. R. Chen, J. N. Leboeuf, A. A. Puretzky, and D. B. Geohegan, Phys. Rev. Lett. **79**, 1571 (1997).
[33]D. Yadav, V. Gupta, and R. K. Thareja, J. Appl. Phys. **106**, 064903 (2009).
[34]A. Thum-Jaeger, B. K. Sinha, and K. P. Rohr, Phy. Rev. E. **63**, 016405 (2001).